The EMBO Journal Vol.18 No.6 pp.1480–1491, 1999

EFA6, a sec7 domain-containing exchange factor for ARF6, coordinates membrane recycling and actin cytoskeleton organization

Michel Franco[1], Peter J.Peters[2], Joëlle Boretto, Elly van Donselaar[2], Antonino Neri[3], Crislyn D'Souza-Schorey[4] and Philippe Chavrier[5]

Centre d'Immunologie INSERM-CNRS de Marseille-Luminy, Case 906, 13288 Marseille Cedex 9, France, [2]Department of Cell Biology, University of Utrecht Medical School, 3584 Utrecht, The Netherlands, [3]Servizio Ematologia, Ospedale Maggiore IRCCS, Milan, Italy and [4]Department of Biological Sciences and the Walther Cancer Institute, University of Notre Dame, IN 46556, USA

[1]Present address: Institut de Pharmacologie Moléculaire et Cellulaire du CNRS, 660 route des Lucioles, Sophia Antipolis, 06560 Valbonne, France

[5]Corresponding author
e-mail: chavrier@ciml.univ-mrs.fr

We have identified a human cDNA encoding a novel protein, exchange factor for ARF6 (EFA6), which contains Sec7 and pleckstrin homology domains. EFA6 promotes efficient guanine nucleotide exchange on ARF6 and is distinct from the ARNO family of ARF1 exchange factors. The protein localizes to a dense matrix on the cytoplasmic face of plasma membrane invaginations, induced on its expression. We show that EFA6 regulates endosomal membrane recycling and promotes the redistribution of transferrin receptors to the cell surface. Furthermore, expression of EFA6 induces actin-based membrane ruffles that are inhibited by co-expression of dominant-inhibitory mutant forms of ARF6 or Rac1. Our results demonstrate that by catalyzing nucleotide exchange on ARF6 at the plasma membrane and by regulating Rac1 activation, EFA6 coordinates endocytosis with cytoskeletal rearrangements.

Keywords: actin/ARF6/endocytosis/guanine nucleotide exchange factor/Rac1

Introduction

A variety of macromolecules such as ligand-bound receptors, plasma membrane proteins and solutes are internalized by clathrin-dependent or -independent endocytic pathways and are delivered to sorting endosomes (reviewed in Gruenberg and Maxfield, 1995). In the sorting compartment, ligands and receptors destined for degradation are segregated from those that recycle back to the plasma membrane (Ghosh *et al.*, 1994; Hopkins *et al.*, 1994). Recycling to the plasma membrane may occur directly from the sorting endosome (Hopkins *et al.*, 1994; Daro *et al.*, 1996) or via a pericentriolar recycling endosomal compartment (Hopkins *et al.*, 1994). Several Ras-related small G proteins of the Rab subgroup that localize to early endocytic compartments have been implicated in the control of various steps of endocytic trafficking (Novick and Zerial, 1997). More recently, small G proteins belonging to the Rho subgroup have also been implicated in endocytic trafficking and are thought to coordinate the dynamics of the peripheral membrane system and the cortical actin cytoskeleton (Lamaze *et al.*, 1996; Murphy *et al.*, 1996).

In addition to Rab and Rho proteins, members of the ADP-ribosylation factor (ARF) subfamily of small G proteins are thought to function as regulators of membrane trafficking. Several studies have demonstrated that activation of ARF1 is required for recruitment of the clathrin-coat adaptor AP1 and the non-clathrin coat COPI to Golgi membranes (Serafini *et al.*, 1991; Orci *et al.*, 1993; Stamnes and Rothman, 1993; Traub *et al.*, 1993), as well as recruitment of AP3 adaptor complex to endosomal membrane structures (Ooi *et al.*, 1998). Hydrolysis of bound GTP triggers coat disassembly allowing vesicle fusion with the acceptor membrane (Tanigawa *et al.*, 1993). These observations, together with the fact that ARF activation is coupled with phospholipase D (PLD) stimulation (Brown *et al.*, 1993; Cockcroft *et al.*, 1994) have led to the proposal that ARF1 is central to the process of vesicle budding by coordinating coat recruitment and membrane vesiculation with coat disassembly and vesicle fusion (Bednarek *et al.*, 1996). ARF6, on the other hand, the least conserved ARF protein, is associated with and controls the integrity of peripheral membranes and appears to cycle between the plasma membrane and a recycling endosomal compartment depending on its nucleotide status (D'Souza-Schorey *et al.*, 1995, 1998; Peters *et al.*, 1995; Radhakrishna and Donaldson, 1997). In Chinese hamster ovary (CHO) cells, ARF6Q67L, a GTP-bound and constitutively activated mutant of ARF6, is localized to the plasma membrane where it induces extensive membrane invaginations, decreases the rate of transferrin (Tfn) internalization, and triggers a redistribution of Tfn receptors (Tfn-Rs) to the cell surface (D'Souza-Schorey *et al.*, 1995, 1998). In contrast, ARF6T27N is associated with a pericentriolar tubulovesicular compartment that contains Tfn-Rs and cellubrevin, and is morphologically reminiscent of the recycling endosomal compartment (D'Souza-Schorey *et al.*, 1995, 1998; Peters *et al.*, 1995). ARF6 has also been implicated in cortical actin cytoskeleton rearrangements. Expression of ARF6Q67L induces the formation of actin-rich surface protrusions (Radhakrishna *et al.*, 1996; D'Souza-Schorey *et al.*, 1997) that can be inhibited by co-expression of deletion mutants of POR1 (D'Souza-Schorey *et al.*, 1997), a protein initially identified as a partner of the Rho GTP-binding Rac1 (Van Aelst *et al.*, 1996), and which has been shown to interact with activated ARF6. The relationship between ARF6 function and actin cytoskeleton organization is further illustrated by the finding that inhibitors of actin polymerization, such

as cytochalasin D, block ARF6-mediated actin rearrangements and induce a redistribution of ARF6 from the plasma membrane to recycling endosomes (Radhakrishna and Donaldson, 1997). The above observations have led to the speculation that ARF6 activation by GDP/GTP exchange takes place intracellularly on the recycling endosome and drives the recycling of membrane to the cell surface. It has also been postulated that ARF6 controls plasma membrane remodeling by coordinating membrane flow from a pericentriolar recycling compartment with cortical actin organization (Radhakrishna *et al.*, 1996; D'Souza-Schorey *et al.*, 1997; Radhakrishna and Donaldson, 1997). There are several observations that support the conclusion that exit sites of recycling membranes at the cell surface are polarized and correlate with the formation of actin-based structures. For instance, recycling Tfn-Rs are targeted to specialized regions of the plasma membrane at the leading lamellae of migrating fibroblasts and in membrane ruffling areas (Hopkins *et al.*, 1994; Bretscher and Aguado-Velasco, 1998b). Whether and how ARF6 regulation of membrane traffic is coordinated with its effect on actin rearrangements is still unknown. In addition, the site of activation of ARF6 by nucleotide exchange has not yet been determined.

Activation of the low molecular weight GTP-binding proteins is mediated by guanine nucleotide exchange factors (GEFs), which catalyze the replacement of bound GDP with GTP. An important breakthrough toward the identification of GEFs acting on ARF proteins was the cloning of two related ARF1 GEFs encoding genes in yeast, GEA1 and GEA2 (Peyroche *et al.*, 1996). This made possible the cloning of a human cDNA encoding ARNO (ARF nucleotide-binding-site opener), which promotes guanine nucleotide exchange on human ARF1 *in vitro* (Chardin *et al.*, 1996). These three proteins share a conserved region of ~200 amino acids which bears 42% of sequence identity with a portion of the *Saccharomyces cerevisiae* SEC7 gene product (Franzusoff and Schekman, 1989) and is essential for GEF activity (Chardin *et al.*, 1996). Two additional Sec7 domain-containing GEFs have been identified: cytohesin-1 and GRP-1/ARNO3, which show extensive homology with the predicted sequence of ARNO (Liu and Pohajdak, 1992; Klarlund *et al.*, 1997; Franco *et al.*, 1998). Similarities between the three ARNO-family members are not restricted to the conserved Sec7 domain but extend to an N-terminal coiled-coil sequence as well as to a C-terminal pleckstrin homology (PH) domain. This PH domain encodes the high affinity of the GEF for phosphoinositide-3,4,5-trisphosphates [PtdIns-(3,4,5)P_3] (Klarlund *et al.*, 1997) and mediates PtdIns-(4,5)P_2-dependent stimulation of ARNO GEF activity (Chardin *et al.*, 1996). Recently, we analyzed the substrate specificity of the ARNO family members and showed that all three proteins stimulate guanine nucleotide exchange on ARF1 but are inefficient on ARF6, *in vitro* (Franco *et al.*, 1998). Klarlund *et al.* (1998) also reported that GRP-1, the mouse homolog of human ARNO3, does not promote exchange on ARF6. In addition, cytohesin-1 catalyzes nucleotide exchange on ARF1 and ARF3 but not on ARF5 (Meacci *et al.*, 1997). These findings from different laboratories are in contrast with those of Frank *et al.*, who reported that ARNO can catalyze GDP/GTP exchange on ARF6 *in vitro*, although these authors observed that ARNO promotes exchange on ARF6 with a much lower efficiency compared with ARF1 (Frank *et al.*, 1998). Finally, we and others have observed that overexpression of ARNO and ARNO3 results in a fragmentation of the Golgi apparatus and an inhibition of Golgi function without affecting the endocytic pathway (Franco *et al.*, 1998; Monier *et al.*, 1998). Therefore, the regulatory function of ARNO-like GEFs on ARF1 activation appears critical for maintaining the integrity of Golgi structure and for vesicle transport within the Golgi complex. The above findings support the contention that ARNO proteins function as GEFs preferentially for ARF1.

In order to identify GEFs involved in ARF6 activation, we sought to isolate and characterize new Sec7 domain-containing ARF GEFs that could promote nucleotide exchange preferentially on ARF6. By analysis of the database, we have identified a human cDNA encoding a protein that we have designated EFA6 (exchange factor for ARF6), which contains Sec7 and PH domains. EFA6 promotes efficient guanine nucleotide exchange on ARF6 in comparison with ARF1. We have analyzed the subcellular localization of EFA6 in transfected cells and investigated its effect on the peripheral plasma membrane/endosome system. Our results suggest that EFA6 regulates two coordinated activities that remodel the cell periphery: (i) the outward flow of membrane from a recycling endosomal compartment; and (ii) a redistribution of the cortical actin cytoskeleton that may facilitate endosomal membrane delivery to the cell surface. Furthermore, EFA6 expression had no effect on the integrity of the biosynthetic and secretory apparatus.

Results

EFA6 is a GEF for ARF6

We searched the database for new Sec7 domain-related sequences that might code for ARF6-specific GEF(s). Using the amino acid sequence of the ARNO Sec7 domain as bait, a BLAST search (Altschul *et al.*, 1990) identified several sequences homologous to the Sec7 domain of ARNO, including a novel open reading frame encoding a 645 amino acid protein (data not shown). This cDNA clone, originally called PSD and expressed in brain tissues (Perletti *et al.*, 1997), encodes an ARF6 GEF (see below) which we have named EFA6. Adjacent to the Sec7 domain, the predicted sequence of EFA6 contains a PH domain (Figure 1A). Except for the conserved Sec7 and PH domains, EFA6 and ARNO-related GEFs are divergent in primary sequence. As shown in Figure 1A, EFA6 contains proline-rich regions at N- and C-terminal ends and a putative coiled-coil forming sequence at the C-terminus. Amino acid sequence comparison revealed that the Sec7 domain of EFA6 exhibits 28 and 30% amino acid identity with the Sec7 domains of Sec7p and ARNO, respectively, compared with 42% amino acid identity between the Sec7 domain of ARNO and Sec7p. The three-dimensional structure of the Sec7 domain of ARNO (Cherfils *et al.*, 1998; Mossessova *et al.*, 1998) has demonstrated the importance of two conserved motifs within the protein sequence, motifs 1 and 2, which fold to form a hydrophobic groove that has been proposed to interact with the switch regions of ARF1 (Béraud-Dufour *et al.*, 1998; Cherfils *et al.*, 1998; Mossessova *et al.*, 1998). Interestingly, motifs

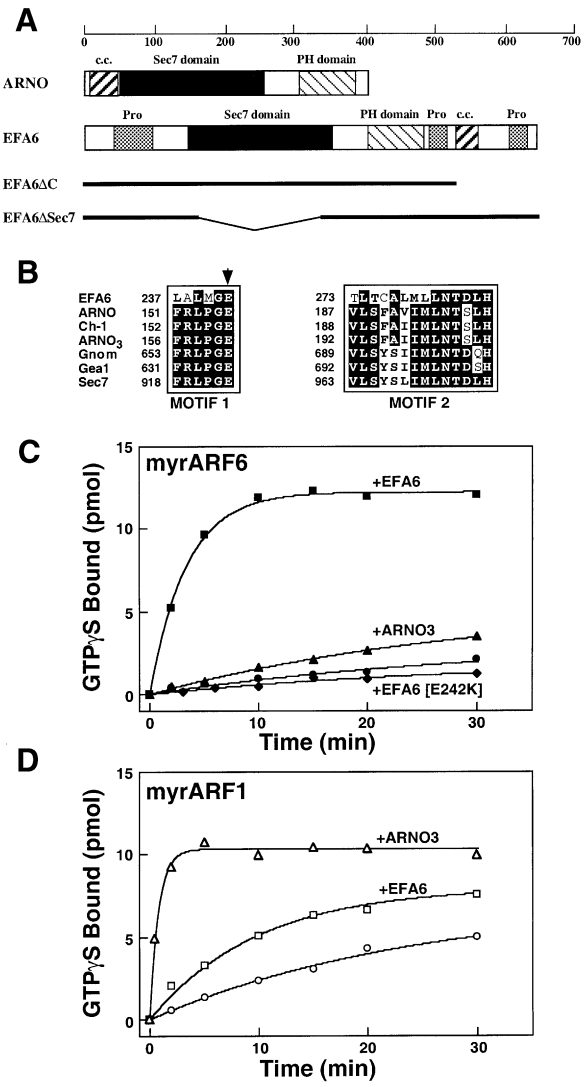

Fig. 1. EFA6 catalyzes guanine nucleotide exchange preferentially on ARF6. (**A**) Schematic representation of ARNO and EFA6. Proline-rich regions (Pro), Sec7 domains, PH domains and coiled-coil regions (c.c.) are shown. Structure of deletion mutants EFA6ΔC and ΔSec7 is depicted. (**B**) Alignment of sequences of two highly conserved motifs of Sec7 domains from human EFA6 (Perletti *et al*., 1997), ARNO (Chardin *et al.*, 1996), cytohesin 1 (Ch-1) (Liu and Pohajdak, 1992), ARNO3 (Franco *et al.*, 1998), *Arabidopsis* GNOM (Shevell *et al.*, 1994), yeast Gea1 (Peyroche *et al.*, 1996) and Sec7 (Achstetter *et al.*, 1988) proteins. These motifs are thought to form a hydrophobic groove that comes in contact with the switch regions of ARF to form the active site of the GEF (Béraud-Dufour *et al.*, 1998; Mossessova *et al.*, 1998). The invariant glutamate residue (ARNO/Glu156 and EFA6/Glu242) which is involved in nucleotide exchange, is indicated with an arrowhead. (**C** and **D**) Measurement of [^{35}S]GTPγS binding to myrARF6 (C) or myrARF1 (D) in the absence (circles) or the presence of purified recombinant EFA6 (squares), EFA6$_{E242K}$ (diamonds) or ARNO3 (triangles). Data shown are representative of three independent experiments.

1 and 2 of the Sec7 domain of EFA6 are the least conserved (Figure 1B), suggesting that its substrate specificity may be distinct from ARNO-related Sec7 domains.

To determine the substrate specificity of EFA6, we measured the ability of recombinant EFA6 to catalyze the binding of guanosine 5′-[γ-thio]triphosphate ([^{35}S]GTPγS) on recombinant myristoylated ARF6 (myrARF6) and myrARF1. As shown in Figure 1C, EFA6-catalyzed binding of [^{35}S]GTPγS to myrARF6 was maximal after 10 min (Figure 1C, closed triangles), whereas ARNO3 was unable to catalyze nucleotide exchange on myrARF6 under the same conditions. Conversely, nucleotide exchange on myrARF1 was rapid and reached a maximal rate within 5 min in the presence of ARNO3, while it was only weakly accelerated in the presence of EFA6 (Figure 1D). Analogous to ARNO-stimulated exchange on myrARF1 (Chardin *et al.*, 1996), EFA6-catalyzed exchange on myrARF6 was unaffected by the addition of brefeldin A (data not shown). Motif 1 of all Sec7 domains identified so far has a conserved glutamate residue (Figure 1B, arrow). Substitution of this glutamate residue by a lysine in the Sec7 domain of ARNO (ARNO$_{E156K}$) reduces its nucleotide exchange activity by at least 1000-fold (Béraud-Dufour *et al.*, 1998; Mossessova *et al.*, 1998). Similarly, EFA6$_{E242K}$ has lost GEF activity indicating that Glu242 of EFA6 is essential for catalytic activity (Figure 1C). Finally, and as already shown for ARNO (Chardin *et al.*, 1996; Franco *et al.*, 1998), the isolated EFA6 Sec7 domain was sufficient to promote nucleotide exchange on ARF6 (data not shown). Therefore, we conclude that EFA6 belongs to the family of Sec7 domain containing ARF GEFs, and is the first ARF6-specific GEF identified so far.

EFA6 localizes to the plasma membrane and induces invaginations

To determine the cellular localization and function of EFA6, we epitope tagged the N-terminal end of EFA6 with the vesicular stomatitis virus glycoprotein (VSV-G) and transiently expressed the protein in TRVb-1 cells [a CHO-derived cell line overexpressing the human Tfn-R (McGraw *et al.*, 1987)]. Confocal immunofluorescence microscopy analysis with anti-VSV-G-tag antibody showed that, analogous to the distribution of ARF6 (Figure 2A), EFA6 localized to membrane ruffles (arrows) and microvilli-like structures (arrowheads) that were induced at the periphery of TRVb-1 cells (Figure 2B). Noticeably, membrane ruffles were more enhanced in EFA6-expressing cells compared with ARF6-transfected cells. Membrane association of overexpressed ARF6 and EFA6 was confirmed by immunoblot analysis of membranes and cytosol of transfected cells, fractionated by high-speed centrifugation. As seen in Figure 2C, immunoblotting with anti-hemagglutinin (HA) tag and anti-EFA6 antibodies revealed protein species of ~22 kDa (ARF6-HA) and ~70 kDa (VSV-G-EFA6), respectively. Both ARF6 and EFA6 were predominantly membrane-bound while only a small fraction of these proteins was present in the soluble fraction. In contrast, deletion of the 241 C-terminal amino acids of EFA6, including the PH domain, led to a protein that was mostly detected in the cytosolic fraction (Figure 1C, VSV-G-EFA6ΔPH), suggesting that the PH domain is required for membrane association of EFA6.

We have studied the peripheral rearrangements induced on EFA6 expression at the ultrastructural level. Cryo-immunogold electron microscopy using antibodies directed against EFA6 revealed that the protein was localized to the plasma membrane, on folds and invaginations, that in cross sections appeared as membrane enclosed structures with an electroluescent lumen (Figure 3A). These structures resembled membrane alterations previously observed in ARF6Q67L-expressing cells (Peters *et al.*, 1995) and that have been shown to be continuous with

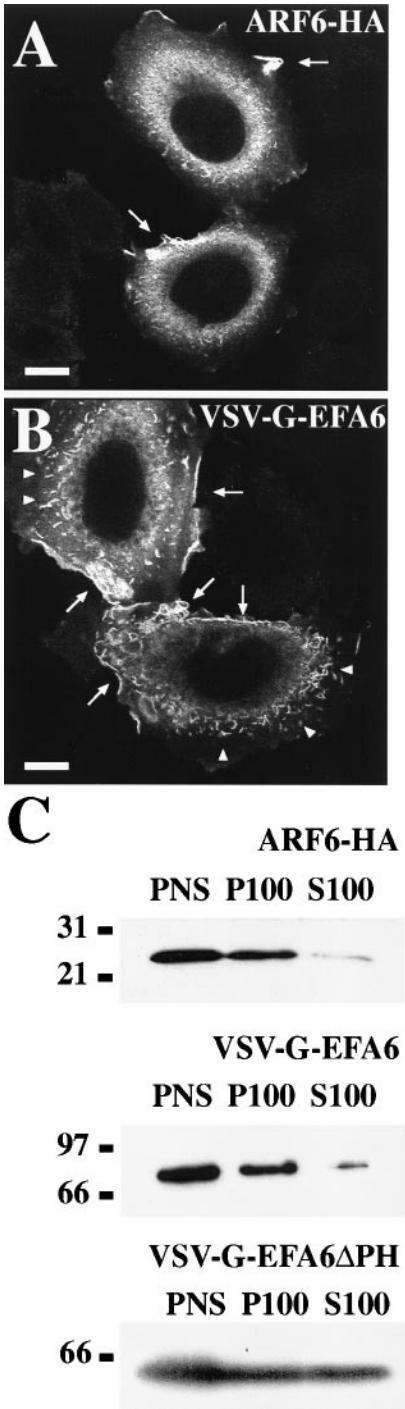

Fig. 2. Localization of overexpressed EFA6 by indirect immunofluorescence microscopy. TRVb-1 cells were grown on coverslips and transfected with expression plasmids encoding HA-tagged ARF6 (**A**) or VSV-G-tagged EFA6 (**B**). Cells were fixed and labeled with either anti-HA (A) or anti-VSV-G (B) epitope antibody. Arrows indicate labeling of plasma membrane ruffles at cell edges. Arrowheads in B point to labeling for EFA6 on microvilli at the dorsal cell surface. Bar, 10 μm. (**C**) The post-nuclear supernatants (PNS) of TRVb-1 cells expressing either ARF6-HA, VSV-G-EFA6 or VSV-G-EFA6ΔPH were centrifuged at 100 000 *g* to give a membrane (P100) and a soluble fraction (S100). Fractions prepared from ARF6-HA-expressing cells were immunoblotted using anti-HA mouse monoclonal antibody (upper panel). Fractions from VSV-G-EFA6 or VSV-G-EFA6ΔPH-expressing cells were incubated with rabbit anti-EFA6 polyclonal antibodies (lower panel). Molecular weights (kDa) of protein markers are indicated.

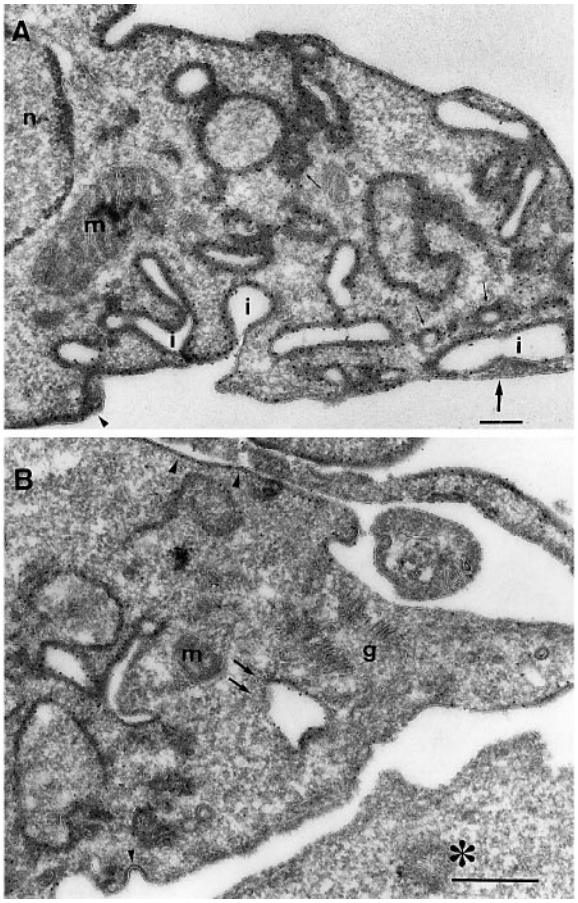

Fig. 3. Localization of EFA6 by electron microscopy. TRVb-1 cells expressing VSV-G-EFA6 were fixed and processed for cryoimmunogold labeling. Sections were labeled with anti-EFA6 antibodies followed by protein A–10 nm gold. (**A**) In TRVb-1 cells overexpressing EFA6, the plasma membrane exhibited extensive membrane invaginations (i). Most of the cytoplasmic face of the plasma membrane was coated by an electron-dense matrix. EFA6 localizes exclusively to this dense matrix (arrowhead) and regions of the plasma membrane with no EFA6 are devoid of matrix (large arrow). Small arrows depict cross sections across tubular structures consisting of a sheath of electron-dense material surrounding a membrane-bound electroluescent lumen. Bar, 200 nm. (**B**) Regions of plasma membrane with little EFA6 labeling show a thinner matrix (large arrowheads). EFA6 labeling is excluded from coated pits (small arrowhead) and caveolae (arrows) as well as from the Golgi region of the cell. m, mitochondria; i, invaginations; n, nucleus; asterisk, untransfected cell. Bar, 500 nm.

the extracellular milieu (D'Souza-Schorey *et al.*, 1998). Strikingly, the cytoplasmic face of the plasma membrane and of EFA6-induced invaginations exhibited a homogenous electron-dense matrix 50 nm thick. This dense material was decorated with anti-EFA6 antibodies indicating that EFA6 was present on this matrix. Regions of plasma membrane showing high levels of labeling with anti-EFA6 antibodies had a thicker matrix (Figure 3A, arrowheads). On the contrary, regions with little EFA6 labeling had only a thin matrix (Figure 3B, large arrowheads) and regions with no labeling were devoid of matrix (Figure 3A, large arrow). Some of the EFA6-positive structures appeared as cross-sections across sheathed cables with an electron-dense sheath surrounding a core electroluescent lumen enclosed within a membrane (Figure 3A, small arrows). This electron-dense matrix

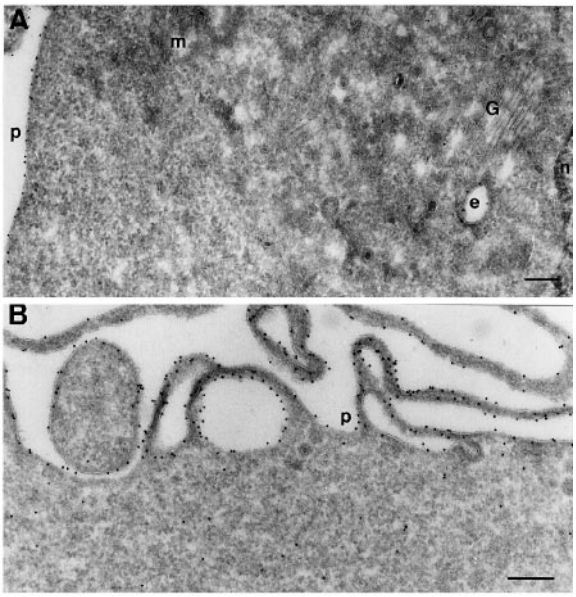

Fig. 4. Plasma membrane association of nucleotide exchange-defective mutant of EFA6. TRVb-1 cells expressing EFA6ΔSec7, which presents a deletion of the entire Sec7 nucleotide exchange domain, were fixed and processed for cryoimmunogold labeling as described in the legend of Figure 3. (**A**) In low-level expressor, EFA6ΔSec7 is localized to the plasma membrane that does not show morphological alteration and is devoid of matrix. Labeling is also detected on intracellular endocytic structures (e). (**B**) In high level expressing cell, EFA6ΔSec7 is associated with the plasma membrane on thin and long extensions. Plasma membrane appears uncoated. EFA6ΔSec7 is also detected in the cytosol. e, endosome; G, Golgi apparatus; m, mitochondria; n, nucleus; p, plasma membrane. Bar, 200 nm.

may represent polymerized actin filaments beneath the surface of plasma membrane invaginations (see below). As shown in Figure 3B, EFA6 label was excluded from clathrin coated pit and caveolae profiles at the plasma membrane and from the Golgi.

In order to investigate whether these morphological effects were dependent on guanine nucleotide exchange catalyzed by EFA6, TRVb-1 cells overexpressing a GEF-defective mutant form of EFA6 were analyzed by cryo-immunogold electron microscopy. Figure 4 shows labeling for EFA6 in TRVb-1 cells expressing low (Figure 4A) or high levels (Figure 4B) of EFA6ΔSec7, a Sec7 domain deletion mutant. In low-level expressors, most of the EFA6 labeling was detected at the plasma membrane, which exhibited normal unperturbed morphology and was devoid of matrix (Figure 4A). Occasionally, EFA6ΔSec7 was also associated with intracellular endocytic structures but was absent from Golgi, nucleus and ER profiles. At a higher level of expression (Figure 4B), EFA6ΔSec7 was localized to the plasma membrane on thin and long extensions that were morphologically distinct from the invaginations seen in wild-type EFA6-expressing cells. The plasma membrane of EFA6ΔSec7-expressing cells was devoid of matrix. Some EFA6ΔSec7 label was also detected in the cytosol. Taken together, these findings indicate that EFA6 localizes predominantly to the plasma membrane and that this distribution is independent of its activity as an ARF6-specific GEF. Plasma membrane association of catalytically active EFA6 induces membrane invaginations and the formation of a dense matrix.

Overexpression of EFA6 inhibits Tfn uptake and affects the distribution of the Tfn-R

Overexpression of ARF6Q67L, a mutant locked in the GTP-bound conformation decreases the rate of Tfn uptake in TRVb-1 cells (D'Souza-Schorey *et al.*, 1995). Since overexpression of EFA6 should increase the pool of ARF6 in a GTP-bound state, we anticipated that the Tfn cycle should be similarly affected in EFA6-transfected cells. To this end, we examined the internalization of fluoresceinated human Tfn in TRVb-1 cells expressing HA-tagged ARF6Q67L. In untransfected cells, Tfn internalized for 20 min at 37°C, accumulated in a single discrete patch in the pericentriolar region of the cells as well as in vesicular structures spread throughout the cytoplasm. Similar to that observed in cells expressing ARF6(Q67L) (Figure 5A), uptake of Tfn was dramatically inhibited in EFA6-expressing cells with little or no accumulation of Tfn after a 20 min incubation (Figure 5B). Conversely, expression of myc-ARNO3, an ARF1 GEF, had no effect on Tfn uptake (Figure 5C), indicating that the inhibitory effect of EFA6 on the Tfn cycle is mediated by activation of ARF6-*in vivo*. Cryoimmunogold labeling with antibodies directed against Tfn-R revealed that in mock-transfected TRVb-1 cells most of the Tfn-R label (74%) resides intracellularly in a tubular and vesicular compartment in the pericentriolar region (Table I). On the contrary, a majority of the Tfn-Rs (79%) were detected on the plasma membrane and on plasma membrane folds and vaginations of TRVb-1 cells expressing EFA6 (Table I). Taken together, these findings indicate that expression of EFA6 induces a redistribution of Tfn-Rs from the perinuclear endosomal recycling compartment to plasma membrane.

In order to investigate whether the effects of EFA6 expression were restricted to the peripheral plasma membrane/endosomal system, we analyzed the intracellular distribution of markers of the secretory and late endocytic pathways in EFA6-expressing cells. The distribution of p23 [a *cis*-Golgi network-associated protein (Rojo *et al.*, 1997)] and of sec61β (a resident ER marker) was not modified by EFA6 overexpression (data not shown). Furthermore, the distribution of the lysosomal marker LAMP-1 remained unperturbed in EFA6-expressing cells (not shown). Thus, expression of EFA6 results in a specific and profound remodeling of the peripheral plasma membrane/endosomal system.

EFA6 overexpression induces rearrangements of the actin cytoskeleton

In addition to the regulation of peripheral membrane trafficking, ARF6 has also been demonstrated to regulate the assembly and organization of the cortical actin cytoskeleton (Radhakrishna *et al.*, 1996; D'Souza-Schorey *et al.*, 1997). These studies, together with our observation that a dense cytoskeletal-like matrix accumulated at the cell surface upon EFA6 expression, prompted us to investigate the consequences of EFA6 expression on the actin cytoskeleton in HeLa cells. We have found that cells expressing wild-type EFA6 showed a marked accumulation of F-actin in peripheral membrane ruffles (Figure 6A). EFA6-induced ruffles at the peripheral edges of the cell were more prominent compared with actin rearrangements observed in ARF6Q67L-expressing cells (not shown). Double labeling for EFA6 with anti-VSV-G tag antibody

Fig. 5. Transferrin accumulation is blocked in EFA6-expressing cells. TRVb-1 cells expressing ARF6Q67L-HA (**A**), VSV-G-EFA6 (**B**) or the ARF1-GEF myc-ARNO3 (**C**) were incubated at 37°C with iron-saturated fluoresceinated human transferrin (FITC–Tfn) for 20 min, fixed and processed for immunofluorescence microscopy. ARF6Q67L, EFA6 and ARNO3 were detected with anti-HA, anti-VSV-G and with anti-myc tag antibodies, respectively. Panels show superimposition of FITC–Tfn with epitope-tagged protein labeling. In untransfected cells, FITC–Tfn is predominantly present in the pericentriolar recycling compartment. In ARF6Q67L- (A) or EFA6-expressing (B) cells there is no accumulation of FITC–Tfn. In contrast, overexpressed ARNO3 (C) has no effect on Tfn distribution. Bar, 10 μm.

revealed that EFA6 co-localized with F-actin in the membrane ruffles (Figure 6B). To determine structural domains of EFA6 involved in peripheral rearrangements, various mutants of EFA6 were transiently expressed in HeLa cells.

Table I. Quantitation of the intracellular distribution of transferrin receptors in control and EFA6-overexpressing TRVb-1 cells

TRVb-1 cells	Plasma membrane and invaginations	Pericentriolar vesicles and tubules
Mock-transfected	26%	74%
EFA6-transfected	79%	21%

TRVb-1 cells on monolayers were mock-transfected or transfected with EFA6-expressing vector, fixed and processed for cryoimmunogold labeling and labeled with anti-EFA6 antiserum followed by protein A–10 nm gold. The data presented represent percentages of 10 nm gold particle count of the total number of gold particles per cell, obtained from 40 random cross-sections of cells.

First, expression of the GEF-defective mutant, $EFA6_{E242K}$ (see Figure 1C), did not induce membrane ruffling, but instead led to the formation of numerous actin-rich membrane extensions (Figure 6C, arrowheads). Similarly, expression of EFA6ΔSec7 also resulted in plasma membrane extensions (Figure 6E and F). EFA6ΔSec7 and $EFA6_{E242K}$ localized predominantly at the cell surface, confirming the ultrastructural analysis (Figure 4). Expression of a C-terminal deletion mutant, EFA6ΔC, generated by deletion of the 124 C-terminal amino acids of EFA6, including a putative coiled-coil sequence and proline-rich region (Figure 1A), abolished the capacity of EFA6 to trigger F-actin reorganization (Figure 6G and H). Furthermore, deletion of this C-terminal region in $EFA6_{E242K}$ ($EFA6_{E242K}\Delta C$) also abolished membrane extension formation (Figure 6I and J), suggesting that the C-terminal domain may be required for interaction with other factors required for cytoskeletal rearrangements. Altogether, these results indicate that EFA6-induced membrane ruffling depends on a functional Sec7 domain and an intact C-terminal end.

The Rho GTP-binding protein, Rac1, is involved in EFA6-induced cytoskeletal rearrangements

Co-expression of EFA6 and ARF6T27N abolished EFA6-mediated membrane ruffling in doubly transfected HeLa cells (Figure 7A and B). Interestingly, these cells exhibited membrane extensions similar to those observed in cells expressing EFA6 mutants defective in GEF activity. These extensions were absent in HeLa cells expressing only ARF6T27N (not shown). Since the Rho-family proteins Rac1 and CDC42 regulate the organization of actin filaments at the cell cortex to induce membrane ruffling and filopodium formation, respectively, we investigated the effects of the dominant-negative mutants of these proteins on EFA6-induced ruffling. When EFA6 was co-expressed with GDP-bound Rac1T17N, membrane ruffling was inhibited and co-transfected cells exhibited numerous F-actin rich membrane extensions **(**Figure 7C and D) that were not detected in cells transfected with Rac1N17 only (not shown). On the contrary, co-expression of EFA6 with GDP-bound CDC42T17N had no effect on EFA6-induced membrane ruffling (Figure 7E and F, arrows). In addition, expression of CDC42N17 had no effect on membrane extensions induced upon expression of the GEF-defective mutants, $EFA6_{E242K}$ and EFA6ΔSec7 (data not shown). These results suggest that EFA6-induced membrane ruffling is independent of CDC42 and that

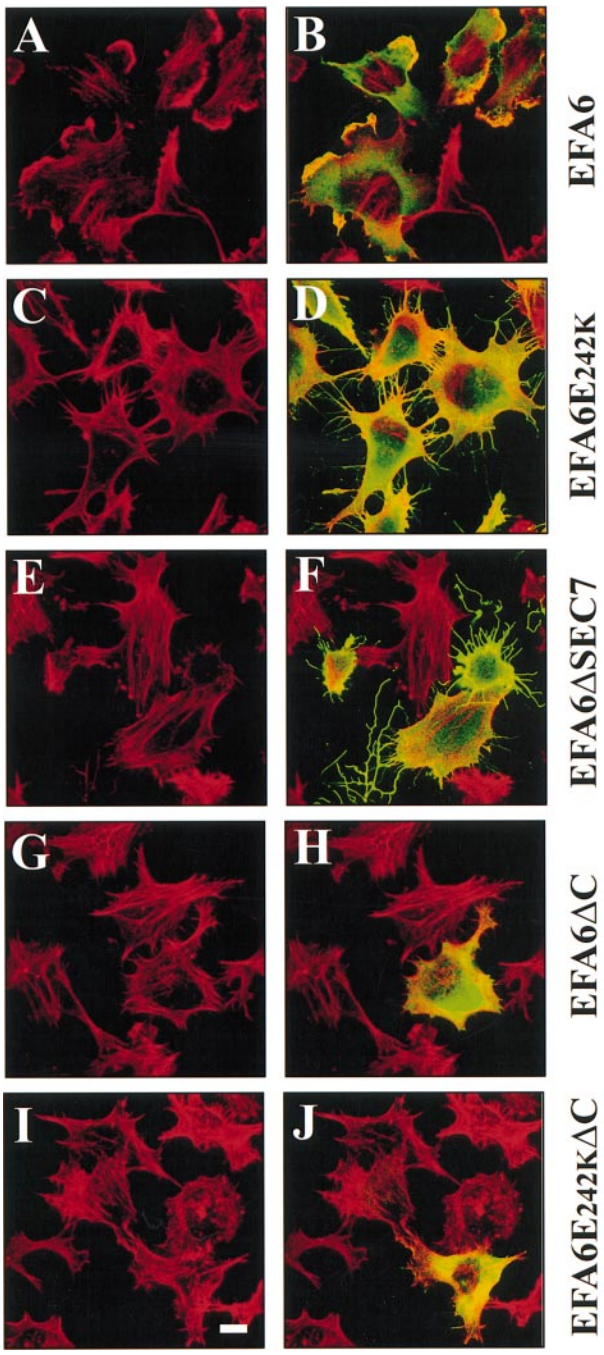

Fig. 6. Effects of EFA6 and EFA6 mutants on actin cytoskeleton rearrangements. HeLa cells were transfected VSV-G-tagged wild-type EFA6 (**A**, **B**), the nucleotide exchange-defective mutants $EFA6_{E242K}$ (**C**, **D**) and EFA6ΔSec7 (**E**, **F**), the C-terminal deletion mutant EFA6ΔC (**G**, **H**) and the double mutant $EFA6_{E242K}$ΔC (**I**, **J**). After 40 h, cells were fixed and labeled with Texas Red-conjugated phalloidin to visualize actin rearrangements (left panels). Right panels show the superimposition of the phalloidin labeling (red) and anti-VSV-G staining (green). Cells overexpressing EFA6 exhibit increased staining for F-actin in membrane ruffles (A). EFA6 colocalizes with F-actin in these ruffles (B). Overexpression of GEF-defective mutant forms, $EFA6_{E242K}$ (C, D) and EFA6ΔSec7 (E, F), induces the extension of filopodia. Deletion of the C-terminal region of EFA6 abolishes EFA6-induced membrane ruffling (G, H) and $EFA6_{E242K}$-mediated filopodia extension (I, J). Bar, 10 μm.

EFA6 triggers the activation of Rac1 which is required for EFA6-induced membrane ruffling. However, it should be noted that EFA6 did not catalyze nucleotide exchange on Rac1 *in vitro*, as shown using the nucleotide exchange assay described above (data not shown).

The effect of EFA6 on Tfn cycling is independent of EFA6-mediated cytoskeletal reorganization

We were interested in determining whether the regulatory activity of EFA6 on membrane dynamics was dependent on EFA6-induced actin cytoskeleton reorganization. To this end, TRVb-1 cells expressing EFA6ΔC, which does not affect F-actin distribution, were incubated with fluoresceinated Tfn for 20 min. As shown above for wild-type EFA6, overexpression of EFA6ΔC prevented intracellular accumulation of Tfn (compare Figure 5A with 8A). In contrast, cells expressing $EFA6_{E242K}$ΔC, a double mutant defective for GEF activity, did not perturb Tfn endocytosis and the distribution of internalized Tfn was similar to that observed in untransfected cells (Figure 8B). Thus, the effects of EFA6 on Tfn cycling requires ARF6 activation by a functional Sec7 domain but is independent of EFA6-induced actin cytoskeleton remodeling which appears to require the C-terminal end of EFA6.

Discussion

In contrast to the other ARF family members that are associated with the secretory pathway (Donaldson and Klausner, 1994; P.J.Peters, unpublished observations), ARF6 is associated with the peripheral plasma membrane/endosome system where it regulates membrane trafficking from an internal fusion competent recycling compartment to the plasma membrane (D'Souza-Schorey *et al.*, 1995, 1998; Peters *et al.*, 1995; Radhakrishna and Donaldson, 1997). Overexpression studies have led to the proposal that ARF6 activation by GDP/GTP exchange is required for the delivery of membrane to the cell surface (Radhakrishna and Donaldson, 1997; D'Souza-Schorey *et al.*, 1998). Recycling to the surface would be facilitated by remodeling of the underlying actin cytoskeleton that is also dependent on ARF6 activation (D'Souza-Schorey *et al.*, 1997; Radhakrishna and Donaldson, 1997). Since ARF6T27N, a mutant thought to be locked in the GDP-bound conformation, localized to the recycling compartment, it was speculated that ARF6 activation takes place intracellularly, on the recycling compartment itself or on putative recycling vesicle intermediates en route to the cell surface (Radhakrishna and Donaldson, 1997; D'Souza-Schorey *et al.*, 1998). However, this model was still speculative due to the lack of an ARF6-GEF. In the present study, we describe a new Sec7 domain containing GEF, EFA6, which promotes efficient GDP/GTP exchange on ARF6. In addition to EFA6, mammalian cells express three highly related GEFs, ARNO, cytohesin-1 and ARNO3/GRP-1, and a 200-kDa GEF, all of which contain a Sec7 domain and promote preferential GDP/GTP exchange on ARF1 (and ARF3) (Chardin *et al.*, 1996; Meacci *et al.*, 1997; Morinaga *et al.*, 1997; Franco *et al.*, 1998; Klarlund *et al.*, 1998). Thus, EFA6 is the first ARF6-specific GEF reported to date. We show that exogenous EFA6 is associated with a dense matrix underlying plasma membrane domains that are extensively invaginated. Plasma membrane alterations induced on EFA6 expression are accompanied by a reorganization of cortical

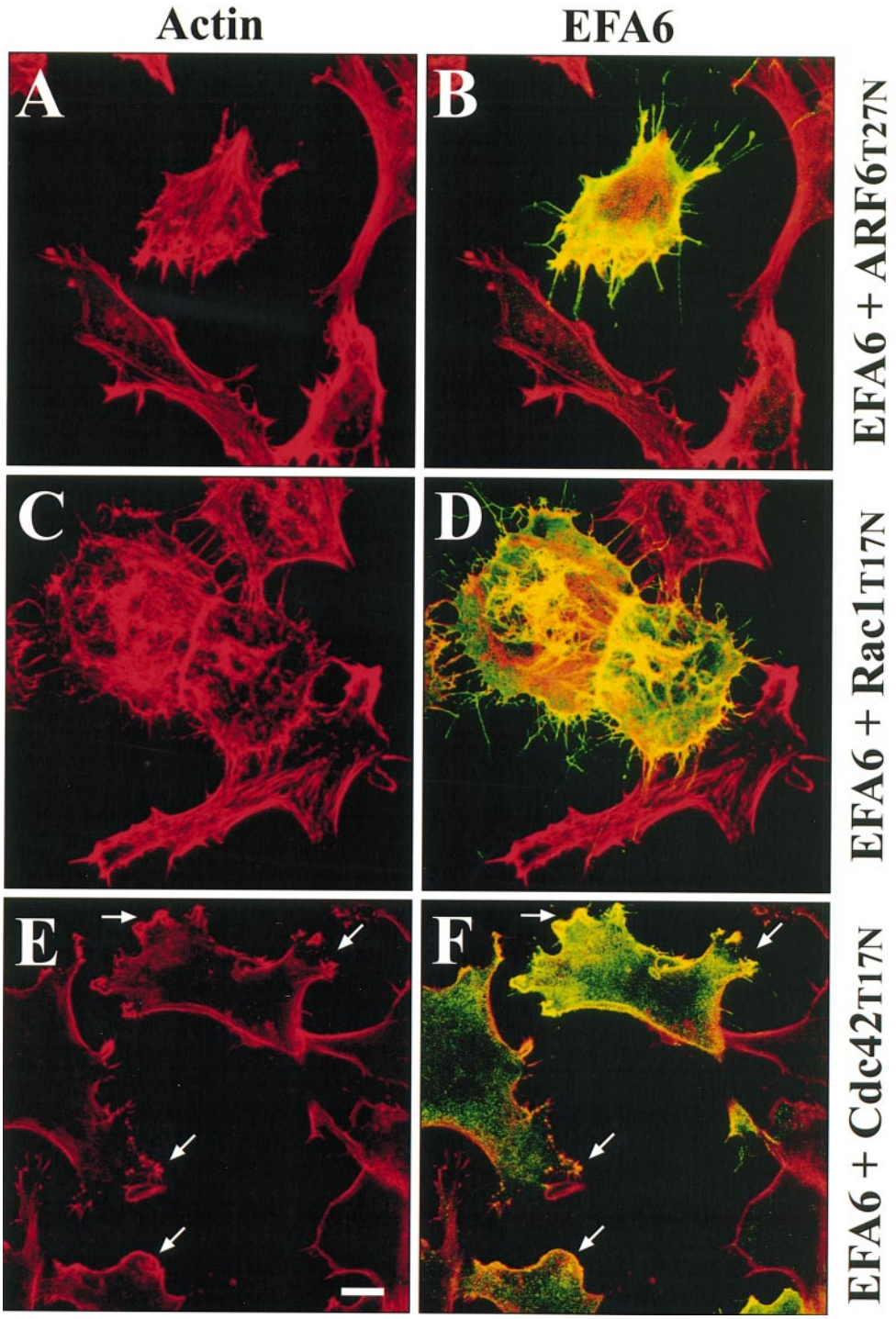

Fig. 7. Rac1 is involved in EFA6-induced actin rearrangements. HeLa cells were co-transfected with constructs expressing VSV-G-EFA6 in combination with ARF6T27N-HA (**A**, **B**), myc-Rac1T17N (**C**, **D**) or myc-CDC42T17N (**E**, **F**). Left panels show Texas Red–phalloidin staining of F-actin. Right panels show superimposition of Texas Red–phalloidin labeling and anti-VSV-G tag labeling. In contrast to EFA6 which induces membrane ruffling (see Figure 9A and B), coexpression of EFA6 together with ARF6T27N (A, B) or Rac1T17N (C, D) leads only to filopodia extension. Cdc42T17N does not affect EFA6-induced membrane ruffling (E and F, arrows). Bar, 10 μm.

actin, with the formation of membrane ruffles. The latter response appears to involve activation of the Rho protein, Rac1. Consistent with previous observations in cells expressing a constitutively activated mutant of ARF6, (ARFQ67L), EFA6 expression affects the Tfn cycle and is accompanied by a redistribution of Tfn-R from the recycling compartment to the cell periphery. These results suggest that EFA6 coordinates membrane and actin remodeling by catalyzing GDP/GTP exchange on ARF6 and by activating Rac1, respectively.

At the ultrastructural level, overexpressed EFA6 was found exclusively on the cytoplasmic side of the plasma membrane and on numerous plasma membrane invaginations that were induced on EFA6 expression. Furthermore, the effects of EFA6 on membrane traffic and organelle structure were restricted to the endosomal and plasma

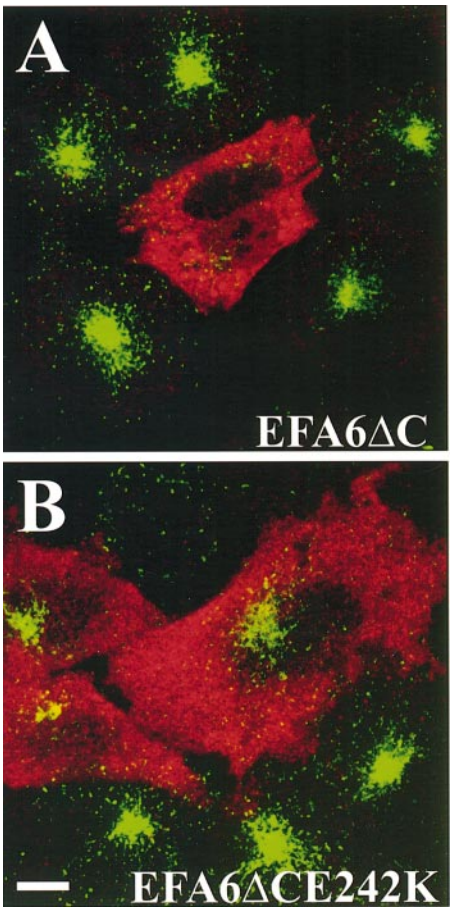

Fig. 8. EFA6-mediated inhibition of Tfn accumulation does not require EFA6-induced actin cytoskeleton reorganization but requires a functional Sec7 domain. TRVb-1 cells expressing VSV-G-EFA6ΔC (**A**) or VSV-G-EFA6$_{E242K}$ΔC (**B**) were incubated for 20 min with fluoresceinated transferrin as described in Figure 5. Panels show the superimposition of fluoresceinated Tfn with VSV-G labeling. In EFA6ΔC-expressing cells (A), there is no accumulation of FITC–Tfn. In contrast, overexpression of GEF-defective EFA6$_{E242K}$ΔC (B) has no effect on Tfn uptake. Bar, 10 μm.

membrane system. Indeed, we observed that EFA6 perturbs the Tfn cycle and redistributes TfnR-containing compartments to the cell surface without affecting the morphology of the Golgi apparatus, endoplasmic reticulum and LAMP-1-positive lysosomes. The observation that the distribution of EFA6 is at the plasma membrane has some important implications for the GDP/GTP cycle of ARF6. One possibility was that EFA6-catalyzed exchange takes place on the recycling compartment where GDP-bound ARF6 accumulates (Peters *et al.*, 1995; D'Souza-Schorey *et al.*, 1998). However, according to this proposal, GEF-defective mutants such as EFA6$_{E242K}$ or EFA6ΔSec7 should accumulate on recycling endosome together with GDP-bound ARF6. Cryoimmunogold electron microscopy and confocal microscopy analyses contradict this prediction, since overexpressed EFA6$_{E242K}$ and EFA6ΔSec7 have the same distribution as wild-type EFA6 at the plasma membrane, demonstrating that plasma membrane localization of EFA6 does not require GDP/GTP exchange on ARF6. Therefore, our data favor the alternative possibility that EFA6 activates ARF6 at the plasma membrane. In this model, recycling membranes (recycling transport intermediates or the recycling endosome) are incompetent for fusion with the plasma membrane until EFA6 converts ARF6 into its GTP-bound active conformation. The initial step of this cascade requires (i) the close proximity of the two membrane systems and (ii) the activation of ARF6 by EFA6 at the interface between these two membrane systems. Regulation of this step could be achieved by controlling EFA6 recruitment to the cell periphery. The PH domain of EFA6 may play an important role in this process since PH domains have been shown to be required for translocation of protein to the plasma membrane (Lemmon *et al.*, 1997). In agreement with this hypothesis, we have observed that deletion of the PH domain of EFA6 leads to a protein which is mostly cytosolic. Overexpression of EFA6 should induce a massive accumulation of ARF6-GTP at the plasma membrane. Normally, GTP hydrolysis that probably involves a plasma membrane-associated GAP should allow the return of GDP-bound ARF6 to recycling endosomes via the endocytic pathway (D'Souza-Schorey *et al.*, 1998), and EFA6 may be released from the membrane into the cytosol. However, in EFA6-expressing cells, GAP-stimulated GTP hydrolysis may become limiting, preventing membrane internalization and thereby blocking Tfn-R internalization and Tfn uptake as also observed in ARF6Q67L-expressing cells.

An interesting finding from the ultrastructural analysis is that EFA6 induces the formation of and is associated with a dense matrix that coats the cytoplasmic face of plasma membrane invaginations. We have also observed that EFA6 induces the projection of actin-based membrane ruffles in which F-actin and EFA6 co-localize. It is possible that the dense matrix observed by electron microscopy is composed of actin filaments polymerized beneath the plasma membrane. Plasma membrane-associated matrix and invaginations, as well as membrane ruffling formation depends on a functional sec7 domain. In contrast, GEF-defective mutant forms of EFA6 lead to the projection of long actin-rich membrane extensions. Consistent with this finding, extensions are also induced upon co-expression of EFA6 and ARF6T27N that should result in dominant inhibition of EFA6 exchange activity. Moreover, co-expression of EFA6 with Rac1T17N, a dominant-inhibitory mutant of Rac1, also results in membrane extension. Finally, deletion of the carboxy end of EFA6 abolished EFA6-induced actin cytoskeleton reorganization. Based on these observations, it is tempting to speculate how EFA6 could control actin cytoskeleton reorganization via the coordinated activation of ARF6 and Rac1 (Figure 9). We propose that Sec7 domain-catalyzed nucleotide exchange on ARF6 allows the engagement of specific effectors such as PLD, which is stimulated by ARF6 *in vitro* (Massenburg *et al.*, 1994) and *in vivo* during exocytosis in chromaffin cells (Caumont *et al.*, 1998). PLD may be involved in membrane dynamics at the interface between plasma membrane and recycling endosome by stimulating the production of fusogenic lipids. On the other hand, GTP-bound ARF6 has been shown to interact with POR1 (D'Souza-Schorey *et al.*, 1997), a protein initially identified as a Rac1 effector involved in membrane ruffling (Van Aelst *et al.*, 1996). Since Rac1T17N does not inhibit ARFQ67L-induced actin rearrangement (D'Souza-Schorey *et al.*, 1997), it is likely that ARF6 and Rac1 are not engaged in a linear pathway

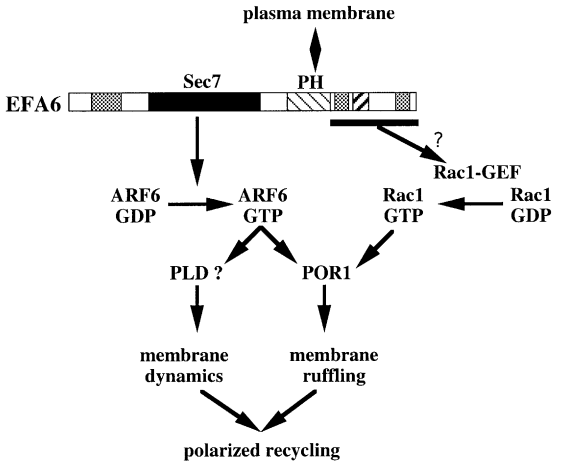

Fig. 9. Model of EFA6-regulated actin reorganization. We propose that targeting of the PH domain of EFA6 to the plasma membrane allows Sec7 domain-catalyzed nucleotide exchange on ARF6. GTP-bound ARF6 interacts with and activates specific downstream effectors at the plasma membrane. Activation of PLD leads to the generation of fusogenic lipids involved in the fusion of recycling membranes with the plasma membrane. In parallel, EFA6 allows Rac1 activation by recruiting a Rac1-specific GEF. The ARF6 and Rac1 pathways converge at the level of POR1 that interacts with both GTP-bound ARF6 and Rac1 to control membrane ruffling. Recycling of membrane occurs at discrete sites of the plasma membrane that coincide with areas of membrane ruffling. The different domains of EFA6 are schematically represented as in Figure 1A.

(ARF6-GTP promoting Rac1 activation), but are rather functioning on parallel pathways that may converge at the level of POR1. Noticeably, ARF6Q67L stimulates actin reorganization but does not induce the formation of the dense matrix we observed in EFA6-expressing cells (Peters *et al.*, 1995; D'Souza-Schorey *et al.*, 1998). An interpretation of these remarkable phenotypic differences may be that the mere engagement of the ARF6-dependent pathway by ARF6Q67L, in the absence of Rac1 engagement, leads only to a partial response. Since EFA6 does not catalyze nucleotide exchange on the Rho-family proteins (M.Franco and P.Chavrier, unpublished observations), we propose that EFA6-dependent Rac1 activation is mediated by a Rac1-specific GEF. A possibility is that the C-terminus of EFA6 which contains coiled-coil and Pro-rich regions known to participate in protein–protein interactions, regulates this Rac1 GEF. Hence, deletion of the C-terminus of EFA6 by prevention of Rac1 engagement would inhibit the actin-based ruffling response. Exocytosis of recycling membrane occurs at the leading edge of migrating cells (Hopkins *et al.*, 1994; for a review see Bretscher and Aguado-Velasco, 1998a). Recently, EGF treatment of KB cells has been shown to induce the formation of membrane ruffles that are enriched in Tfn-Rs, and Tfn-Rs are also targeted to Rac1-induced membrane ruffles in these cells (Bretscher and Aguado-Velasco, 1998b). We believe that, by its coordinated actions on both Rac1- and ARF6-driven pathways, EFA6 allows to couple membrane ruffling and membrane fusion at discrete sites of the plasma membrane in a polarized fashion.

ARF6 has been shown to co-purify along with chromaffin granules (Galas *et al.*, 1997) and controls exocytosis during regulated secretion in chromaffin cells (Caumont *et al.*, 1998). Rac1 is also implicated in regulated exocytosis in mast cells (Norman *et al.*, 1996; Guillemot *et al.*, 1997), and together with the Rac1-specific GEF, Tiam-1, it affects neuronal morphology (Luo *et al.*, 1996; Kozma *et al.*, 1997; Leeuwen *et al.*, 1997). While ARF6 is ubiquitously expressed (Tsuchiya *et al.*, 1991; Yang *et al.*, 1998), the human PSD gene coding for EFA6 is mainly expressed in brain (Perletti *et al.*, 1997). Whether EFA6, by its coordinated action on ARF6 and Rac1, may be involved in neuronal secretion or axonal elongation is presently unknown, but would be an interesting subject of investigation. By screening for EFA6-like genes, we have isolated a cDNA encoding a Sec7 and PH domain-containing protein showing high similarity with the corresponding domains of EFA6 (M.Franco and B.Chavrier, unpublished). Interestingly, this EFA6-like gene is expressed in a wide range of tissues. The availability of these cDNAs will help in clarifying the function of EFA6-like GEFs in various cell types.

Materials and methods

Cells and antibodies

TRVb-1 cells, a CHO-derived cell line overexpressing the human transferrin receptor (McGraw *et al.*, 1987), were grown in Ham's F-12 medium, 5% fetal calf serum (FCS), penicillin/streptomycin, and 100 μg/ml G418. HeLa cells were grown in Dulbecco's modified essential medium supplemented with 10% FCS and antibiotics.

The following antibodies were used for the studies described: mouse monoclonal antibody (mAb) against VSV-G epitope (clone P5D4, Boehringer Mannheim) and rat mAb against HA epitope (clone 3F10, Boehringer Mannheim); mouse mAb against myc epitope (clone 9E10; Evan *et al.*, 1985); mouse mAb anti-Tfn-R (clone H68.4; Zymed, CA); rabbit antiserum against p23 (Rojo *et al.*, 1997); rabbit antiserum against Sec61β (provided by R.Hendriks, ZMBH, Heidelberg, Germany); rabbit antiserum against LAMP-1 (provided by S.Meresse, CIML, Marseille, France); and anti-EFA6 rabbit antiserum raised against the purified recombinant protein.

Construction of EFA6 expression plasmids

EFA6 was cloned from a human brain cDNA library (Clontech) by high fidelity PCR using two oligonucleotide primers; 5′EFA6 primer (5′-GATCGATCCATATGCCTCTCAAGTCACCTG-3′), which contains a *Nde*I linker, the ATG start codon and 5′ nucleotides of EFA6, and 3′EFA6 primer (5′-GGGCGGCGGAAGCCCTGAGTCAACGGATCCTAAGTACA-3′), which contains a *Bam*HI linker, TAG stop codon and 3′ complementary nucleotide residues of EFA6. Primer sequences encoding EFA6 were designed from the published human PSD sequence (Perletti *et al.*, 1997). The PCR product was inserted into pGEM1 and pSRα expression vectors with a N-terminal VSV-G tag using *Nde*I and *Bam*HI restriction sites.

$EFA6_{E242K}$ was constructed by two-stage overlap-extension PCR. The first-stage reaction products were generated using complementary overlapping end primers containing an oligonucleotide-directed point mutation; the N-terminal product was generated with the 5′EFA6 primer described above and the primer 5′-CCTGGGTCTTACCCATTAAG-3′ (EFA6E242K-1). The C-terminal product was generated with the primer 5′-CTTAATGGGTAAGACCCAGG-3′ (EFA6E242K-2) and the 3′EFA6 primer. EFA6 cDNA was used as template. Second-stage PCR was carried out with first-stage reaction products to anneal the overlapping ends, followed by amplification. The full-length EFA6E242K PCR product was cloned in the *Nde*I and *Bam*HI restriction sites of pGEM1VSV-G and pSRαVSV-G expression vectors.

EFA6ΔC and $EFA6_{E242K}$ΔC were constructed by PCR amplification of corresponding EFA6 and $EFA6_{E242K}$ cDNAs in pGEM1VSV-G using the 5′EFA6 primer and the primer 5′-TGTACTAAAGCTTCTACTGGGAGAGGCGGGTGG-3′ (EFA6ΔC) obtained by substituting glutamate 522 of EFA6 with a stop codon. Similarly, EFA6ΔPH was obtained by PCR using the 5′EFA6 primer and the primer 5′-TGTCTAAAGCTTTCAGCCCCGCTTGCCCCGAGG-3′ (EFA6ΔPH) substituting tryptophane 404 of EFA6 with a stop codon. $EFA6\Delta_{Sec7}$ was constructed by two-stage PCR amplification of EFA6 with the 5′EFA6 primer and the primer 5′-GTCGGCCAACTCAGACAGGCTGTCCAGCTCTGAGTC-3′ (EFA6-S156), and with the primer 5′-GACTCAGAGCTGGAC-

AGCCTGTCTGAGTTGGCCGAC-3′ (EFA6-S340) and the 3′EFA6 primer. These PCR products were then amplified with the 5′ and 3′ primers of EFA6 to create an internal deletion from amino acids 157 to 341. The resulting PCR product was subcloned into the *Nde*I and *Bam*HI restriction sites of pGEM1VSV-G.

Expression plasmids used in this study encoding ARF6-HA, ARF6Q67L-HA, ARF6T27N-HA (Peters *et al.*, 1995), mycRac1N17, mycCDC42N17 (Dutartre *et al.*, 1996) and mycARNO3 (Franco *et al.*, 1998) were as described previously.

[^{35}S]GTPγS binding assay

Myristoylated ARF1 and ARF6 were produced and purified as described previously (Franco *et al.*, 1995). Recombinant EFA6 and ARNO3 were produced from pET3a-transformed BL21 (DE3) *Escherichia coli* as described previously (Franco *et al.*, 1998). For [^{35}S]GTPγS binding, measurements were carried out as follows: MyrARF1 or myrARF6 (1 μM) were incubated at 37°C in 50 mM HEPES–NaOH pH 7.5, 1 mM $MgCl_2$, 1 mM dithiothreitol (DTT), 100 mM KCl, 10 μM [^{35}S]GTPγS (~1000 c.p.m./pmol, NEN) supplemented with azolectin vesicles (1.5 g/l, Sigma). Soluble bacterial protein lysates containing EFA6 or ARNO3 were added to a final concentration of 40 μg/ml of total proteins. The estimated GEF concentration in the assay was ~100–200 nM. At indicated time intervals, aliquots of of 25 μl were measured for radioactivity as described previously (Franco *et al.*, 1995).

Internalization of FITC-conjugated transferrin

CHO cells plated on 11 mm round glass coverslips were transiently transfected with pSRα constructs using the Fugene 6 transfection reagent as described by the manufacturer (Boehringer Mannheim). Forty hours after transfection, cells were pre-incubated in serum-free medium containing 1% bovine serum albumin (BSA) for 30 min at 37°C and then incubated for 20 min in the same medium supplemented with 50 μg/ml of iron-loaded FITC-conjugated human transferrin (Molecular Probe). Cells were then washed once in ice-cold phosphate-buffered saline (PBS), fixed in 3% paraformaldehyde and processed for immunofluorescence analysis as described previously (Franco *et al.*, 1998). Confocal microscopy was carried out with a Leica TCS 4D microscope equipped with a mixed gas Argon/Krypton laser (Leica Laser Teknik).

Actin cytoskeleton analysis

HeLa or TRVb-1 cells plated on 11 mm round glass coverslips were infected with T7 RNA polymerase recombinant vaccinia virus (VT7) (Fuerst *et al.*, 1986) and then transfected with pGEM constructs using the Lipofectamine Reagent (Gibco-BRL) as described previously (Guillemot *et al.*, 1997). Four hours after transfection cells were fixed in 3% paraformaldehyde, stained with Texas Red–phalloidin (Molecular Probes), and then processed for immunofluorescence analysis (Franco *et al.*, 1998). For co-transfection experiments, we used ARF6T27N-, Rac1N17- or CDC42N17-encoding constructs in twice the amount as compared with EFA6-encoding plasmid. Co-transfection efficiency was >95% as judged by double labeling with anti-EFA6 and anti-HA (ARF6T27N) or anti-myc (Rac1N17 and CDC42N17) antibodies.

Cryoimmunogold electron microscopy procedures

Cells were fixed, scraped and collected. Cells were then embedded in gelatin and processed for cryosectioning as described previously (D'Souza-Schorey *et al.*, 1998). Ultrathin cryosections were cut at –120°C in a cryo-ultramicrotome (Leica), transferred onto formvar-coated copper grids, and processed for cryoimmunogold labeling as described (D'Souza-Schorey *et al.*, 1998). Briefly, sections were incubated with primary antibody (anti-EFA6 or anti-Tfn-R), followed by incubation with protein A–gold. Labeled sections were contrasted with uranyl, embedded in cellulose and viewed with a JOEL 1010 electron microscope at 80 kV.

Cell fractionation and immunobloting

TRVb-1 cells (5×10^6) were transfected with VSV-G-EFA6- or ARF6-HA-expressing vectors, and 40 h after transfection, cells were washed in phosphate buffer and homogenized in 250 mM sucrose, 3 mM imidazole pH 7.4 with protease inhibitors. The post-nuclear supernatant (PNS) was obtained by centrifugation of the cell lysate at 1000 *g* for 5 min at 4°C. An aliquot of the PNS was further centrifuged for 45 min at 100 000 *g* to separate membrane and cytosolic fractions. Aliquots of the PNS, the membrane pellet and cytosol fractions were loaded on SDS–PAGE and analyzed by Western blotting using anti-HA and anti-EFA6 antibodies to detect ARF6 and EFA6 expression, respectively.

Acknowledgements

We are indebted to J.Gruenberg, R.Hendriks and S.Méresse for generously providing antibodies for this study. We are grateful for the skillful work of the dark room assistance at Utrecht University. P.Chardin, M.Chabre and M.Zerial are thanked for helpful comments on this manuscript. We thank B.Antonny for sharing results prior to publication. This work was supported by INSERM and CNRS institutional funding and specific grants from La Ligue Nationale contre le Cancer and Le Groupement des Entreprises Françaises dans la Lutte contre le Cancer (to P.C.), by grants from the Dutch Cancer Society (to P.J.P.) and a grant from the Associazione Italiana Ricerca sul Cancro (to A.N.). M.F. was supported by a postdoctoral fellowship from the Fondation pour la Recherche Médicale. C.D.-S. is a Leukemia Society of America Special Fellow.

References

Achstetter,T., Franzusoff,A., Field,C. and Schekman,R. (1988) SEC7 encodes an unusual, high molecular weight protein required for membrane traffic from the yeast Golgi apparatus. *J. Biol. Chem.*, **263**, 11711–11717.

Altschul,S.F., Gish,W., Miller,W., Myers,E.W. and Lipman,D.J. (1990) Basic local alignment search tool. *J. Mol. Biol.*, **215**, 403–410.

Bednarek,S.Y., Orci,L. and Schekman,R. (1996) Traffic COPs and the formation of vesicle coats. *Trends Cell Biol.*, **6**, 468–473.

Béraud-Dufour,S., Robineau,S., Chardin,P., Paris,S., Chabre,M., Cherfils,J. and Antonny,B. (1998) A glutamic finger in the guanine nucleotide exchange factor ARNO displaces Mg^{2+} and the β-phosphate to destabilize GDP on ARF1. *EMBO J.*, **17**, 3651–3659.

Bretscher,M.S. and Aguado-Velasco,C. (1998a) Membrane traffic during cell locomotion. *Curr. Opin. Cell Biol.*, **10**, 537–541.

Bretscher,M.S. and Aguado-Velasco,C. (1998b) EGF induces recycling membrane to form ruffles. *Curr. Biol.*, **8**, 721–724.

Brown,H.A., Gutowski,S., Moomaw,C.R., Slaughter,C. and Sternweis, P.C. (1993) ADP-ribosylation factor, a small GTP-dependent regulatory protein, stimulates phospholipase D activity. *Cell*, **75**, 1137–1144.

Caumont,A.S., Galas,M.C., Vitale,N., Aunis,D. and Bader,M.F. (1998) Regulated exocytosis in chromaffin cells. Translocation of ARF6 stimulates a plasma membrane-associated phospholipase D. *J. Biol. Chem.*, **273**, 1373–1379.

Chardin,P., Paris,S., Antonny,B., Robineau,S., Béraud-Dufour,S., Jackson,C.L. and Chabre,M. (1996) A human exchange factor for ARF contains Sec7- and pleckstrin-homology domains. *Nature*, **384**, 481–484.

Cherfils,J., Menetrey,J., Mathieu,M., Le Bras,G., Robineau,S., Beraud-Dufour,S., Antonny,B. and Chardin,P. (1998) Structure of the Sec7 domain of the Arf exchange factor ARNO. *Nature*, **392**, 101–105.

Cockcroft,S. *et al.* (1994) Phospholipase D: a downstream effector of ARF in granulocytes. *Science*, **263**, 523–526.

Daro,E., Van der Sluijs,P., Galli,T. and Mellman,I. (1996) Rab4 and cellubrevin define different early endosome populations on the pathway of transferrin receptor recycling. *Proc. Natl Acad. Sci. USA*, **93**, 9559–9564.

Donaldson,J.G. and Klausner,R.D. (1994) ARF: a key regulatory switch in membrane traffic and organelle structure. *Curr. Opin. Cell Biol.*, **6**, 527–532.

D'Souza-Schorey,C., Li,G., Colombo,M.I. and Stahl,P.D. (1995) A regulatory role for ARF6 in receptor-mediated endocytosis. *Science*, **267**, 1175–1178.

D'Souza-Schorey,C., Boshans,R.L., McDonough,M., Stahl,P.D. and Van Aelst,L. (1997) A role for POR1, a Rac1-interacting protein, in ARF6-mediated cytoskeletal rearrangements. *EMBO J.*, **16**, 5445–5454.

D'Souza-Schorey,C., van Donselaar,E., Hsu,V.W., Yang,C., Stahl,P.D. and Peters,P.J. (1998) ARF6 targets recycling vesicles to the plasma membrane: insights from an ultrastructural investigation. *J. Cell Biol.*, **140**, 603–616.

Dutartre,H., Davoust,J., Gorvel,J.P. and Chavrier,P. (1996) Cytokinesis arrest and redistribution of actin-cytoskeleton regulatory components in cells expressing the rho GTPase CDC42Hs. *J. Cell Sci.*, **109**, 367–377.

Evan,G.I., Lewis,G.K., Ramsay,G. and Bishop,J.M. (1985) Isolation of monoclonal antibodies specific for human c-*myc* proto-oncogene product. *Mol. Cell Biol.*, **5**, 3610–3616.

Franco,M., Chardin,P., Chabre,M. and Paris,S. (1995) Myristoylation of ADP-ribosylation factor 1 facilitates nucleotide exchange at physiological Mg^{2+} levels. *J. Biol. Chem.*, **270**, 1337–1341.

Franco,M., Boretto,J., Robineau,S., Monier,S., Goud,B., Chardin,P. and Chavrier,P. (1998) ARNO3, a Sec7-domain guanine nucleotide exchange factor for ADP ribosylation factor 1, is involved in the control of golgi structure and function. *Proc. Natl Acad. Sci. USA*, **95**, 9926–9931.

Frank,S., Upender,S., Hansen,S.H. and Casanova,J.E. (1998) ARNO is a guanine nucleotide exchange factor for ADP-ribosylation factor 6. *J. Biol. Chem.*, **273**, 23–27.

Franzusoff,A. and Schekman,R. (1989) Functional compartments of the yeast Golgi apparatus are defined by the sec7 mutation. *EMBO J.*, **8**, 2695–2702.

Fuerst,T.R., Niles,E.G., Studier,E.G. and Moss,B. (1986) Eukaryotic transient-expression system based on recombinant vaccinia virus that synthesizes bacteriophages T7 RNA polymerase. *Proc. Natl Acad. Sci. USA*, **83**, 8122–8126.

Galas,M.C., Helms,J.B., Vitale,N., Thierse,D., Aunis,D. and Bader,M.F. (1997) Regulated exocytosis in chromaffin cells. A potential role for a secretory granule-associated ARF6 protein. *J. Biol. Chem.*, **272**, 2788–2793.

Ghosh,R., Gelman,D. and Maxfield,F. (1994) Quantification of low density lipoprotein and transferrin endocytic sorting in HEp2 cells using confocal microscopy. *J. Cell Sci.*, **107**, 2177–2189.

Gruenberg,J. and Maxfield,F.R. (1995) Membrane transport in the endocytic pathway. *Curr. Opin. Cell Biol.*, **7**, 552–563.

Guillemot,J.C., Montcourrier,P., Vivier,E., Davoust,J. and Chavrier,P. (1997) Selective control of membrane ruffling and actin plaque assembly by the Rho GTPases Rac1 and CDC42 in Fc εRI-activated rat basophilic leukemia (RBL-2H3) cells. *J. Cell Sci.*, **110**, 2215–2225.

Hopkins,C.R., Gibson,A., Shipman,M., Strickland,D.K. and Trowbridge,I.S. (1994) In migrating fibroblasts, recycling receptors are concentrated in narrow tubules in the pericentriolar area and then routed to the plasma membrane of the leading lamella. *J. Cell Biol.*, **125**, 1265–1274.

Klarlund,J.K., Guilherme,A., Holik,J.J., Virbasius,J.V., Chawla,A. and Czech,M.P. (1997) Signaling by phosphoinositide-3,4,5-trisphosphate through proteins containing pleckstrin and Sec7 homology domains. *Science*, **275**, 1927–1930.

Klarlund,J.K., Rameh,L.E., Cantley,L.C., Buxton,J.M., Holik,J.J., Sakelis,C., Patki,V., Corvera,S. and Czech,M.P. (1998) Regulation of GRP1-catalyzed ADP ribosylation factor guanine nucleotide exchange by phosphatidylinositol 3,4,5-trisphosphate. *J. Biol. Chem.*, **273**, 1859–1862.

Kozma,R., Sarner,S., Ahmed,S. and Lim,L. (1997) Rho family GTPases and neuronal growth cone remodelling: relationship between increased complexity induced by Cdc42Hs, Rac1 and acetylcholine and collapse induced by RhoA and lysophosphatidic acid. *Mol. Cell. Biol.*, **17**, 1201–1211.

Lamaze,C., Chuang,T.H., Terlecky,L.J., Bokoch,G.M. and Schmid,S.L. (1996) Regulation of receptor-mediated endocytosis by Rho and Rac. *Nature*, **382**, 177–179.

Leeuwen,F.N., Kain,H.E., Kammen,R.A., Michiels,F., Kranenburg,O.W. and Collard,J.G. (1997) The guanine nucleotide exchange factor Tiam1 affects neuronal morphology; opposing roles for the small GTPases Rac and Rho. *J. Cell Biol.*, **139**, 797–807.

Lemmon,M.A., Falasca,M., Ferguson,K.M. and Schlessinger,J. (1997) Regulatory recruitment of signalling molecules to the cell membrane by pleckstrin-homology domains. *Trends Cell Biol.*, **7**, 237–242.

Liu,L. and Pohajdak,B. (1992) Cloning and sequencing of a human cDNA from cytolytic NK/T cells with homology to yeast SEC7. *Biochim. Biophys. Acta*, **1132**, 75–78.

Luo,L., Hensch,T.K., Ackerman,L., Barbel,S., Jan,L.Y. and Jan,Y.N. (1996) Differential effects of the Rac GTPase on Purkinje cell axons and dendritic trunks and spines. *Nature*, **379**, 837–840.

Massenburg,D., Han,J.S., Liyanage,M., Patton,W.A., Rhee,S.G., Moss,J. and Vaughan,M. (1994) Activation of rat brain phospholipase D by ADP-ribosylation factors 1, 5 and 6: separation of ADP-ribosylation factor-dependent and oleate-dependent enzymes. *Proc. Natl Acad. Sci. USA*, **91**, 11718–11722.

McGraw,T.E., Greenfield,L. and Maxfield,F.R. (1987) Functional expression of the human transferrin receptor cDNA in Chinese hamster ovary cells deficient in endogenous transferrin receptor. *J. Cell Biol.*, **105**, 207–214.

Meacci,E., Tsai,S.C., Adamik,R., Moss,J. and Vaughan,M. (1997) Cytohesin-1, a cytosolic guanine nucleotide-exchange protein for ADP-ribosylation factor. *Proc. Natl Acad. Sci. USA*, **94**, 1745–1748.

Monier,S., Chardin,P., Robineau,S. and Goud,B. (1998) Overexpression of the ARF1 exchange factor ARNO inhibits the early secretory pathway and causes the disassembly of the Golgi complex. *J. Cell Sci.*, **111**, 3427–3436.

Morinaga,N., Moss,J. and Vaughan,M. (1997) Cloning and expression of a cDNA encoding a bovine brain brefeldin A-sensitive guanine nucleotide-exchange protein for ADP-ribosylation factor. *Proc. Natl Acad. Sci. USA*, **94**, 12926–12931.

Mossessova,E., Gulbis,J.M. and Goldberg,J. (1998) Structure of the guanine nucleotide exchange factor Sec7 domain of human arno and analysis of the interaction with ARF GTPase. *Cell*, **92**, 415–423.

Murphy,C. *et al.* (1996) Endosome dynamics regulated by a Rho protein. *Nature*, **384**, 427–432.

Norman,J.C., Price,L.S., Ridley,A.J. and Koffer,A. (1996) The small GTP-binding proteins, Rac and Rho, regulate cytoskeletal organization and exocytosis in mast cells by parallel pathways. *Mol. Biol. Cell*, **7**, 1429–1442.

Novick,P. and Zerial,M. (1997) The diversity of Rab proteins in vesicle transport. *Curr. Opin. Cell Biol.*, **9**, 496–504.

Ooi,C.E., Dell'Angelica,E.C. and Bonifacino,J.S. (1998) ADP-Ribosylation factor 1 (ARF1) regulates recruitment of the AP-3 adaptor complex to membranes. *J. Cell Biol.*, **142**, 391–402.

Orci,L., Palmer,D.J., Amherdt,M. and Rothman,J.E. (1993) Coated vesicle assembly in the Golgi requires only coatomer and ARF proteins from the cytosol. *Nature*, **364**, 732–734.

Perletti,L., Talarico,D., Trecca,D., Ronchetti,D., Fracchiolla,N.S., Maiolo,A.T. and Neri,A. (1997) Identification of a novel gene, PSD, adjacent to NFKB2/lyt-10, which contains Sec7 and pleckstrin-homology domains. *Genomics*, **46**, 251–259.

Peters,P.J., Hsu,V.W., Ooi,C.E., Finazzi,D., Teal,S.B., Oorschot,V., Donaldson,J.G. and Klausner,R.D. (1995) Overexpression of wild-type and mutant ARF1 and ARF6: distinct perturbations of nonoverlapping membrane compartments. *J. Cell Biol.*, **128**, 1003–1017.

Peyroche,A., Paris,S. and Jackson,C.L. (1996) Nucleotide exchange on ARF mediated by yeast Gea1 protein. *Nature*, **384**, 479–481.

Radhakrishna,H. and Donaldson,J.G. (1997) ADP-ribosylation factor 6 regulates a novel plasma membrane recycling pathway. *J. Cell Biol.*, **139**, 49–61.

Radhakrishna,H., Klausner,R.D. and Donaldson,J.G. (1996) Aluminum fluoride stimulates surface protrusions in cells overexpressing the ARF6 GTPase. *J. Cell Biol.*, **134**, 935–947.

Rojo,M., Pepperkok,R., Emery,G., Kellner,R., Stang,E., Parton,R.G. and Gruenberg,J. (1997) Involvement of the transmembrane protein p23 in biosynthetic transport. *J. Cell Biol.*, **139**, 1119–1135.

Serafini,T., Orci,L., Amherdt,M., Brunner,M., Kahn,R.A. and Rothman,J.E. (1991) ADP-ribosylation factor is a subunit of the coat of Golgi-derived COP-coated vesicles: a novel role for a GTP-binding protein. *Cell*, **67**, 239–253.

Shevell,D.E., Leu,W.M., Gillmor,C.S., Xia,G., Feldmann,K.A. and Chua,N.H. (1994) EMB30 is essential for normal cell division, cell expansion and cell adhesion in *Arabidopsis* and encodes a protein that has similarity to Sec7. *Cell*, **77**, 1051–1062.

Stamnes,M.A. and Rothman,J.E. (1993) The binding of AP-1 clathrin adaptor particles to Golgi membranes requires ADP-Ribosylation Factor, a small GTP-binding protein. *Cell*, **73**, 999–1005.

Tanigawa,G., Orci,L., Amherdt,M., Ravazzola,M., Helms,J.B. and Rothman,J.E. (1993) Hydrolysis of bound GTP by ARF protein triggers uncoating of Golgi-derived COP-coated vesicles. *J. Cell Biol.*, **123**, 1365–1371.

Traub,L.M., Ostrom,J.A. and Kornfeld,S. (1993) Biochemical dissection of AP-1 recruitment onto Golgi membranes. *J. Cell Biol.*, **123**, 561–573.

Tsuchiya,M., Price,S.R., Tsai,S.C., Moss,J. and Vaughan,M. (1991) Molecular identification of ADP-ribosylation factor mRNAs and their expression in mammalian cells. *J. Biol. Chem.*, **266**, 2772–2777.

Van Aelst,L., Joneson,T. and Bar-Sagi,D. (1996) Identification of a novel Rac1-interacting protein involved in membrane ruffling. *EMBO J.*, **15**, 3778–3786.

Yang,C.Z., Heimberg,H., D'Souza-Schorey,C., Mueckler,M.M. and Stahl,P.D. (1998) Subcellular distribution and differential expression of endogenous ADP-ribosylation factor 6 in mammalian cells. *J. Biol. Chem.*, **273**, 4006–4011.

Received September 7, 1998; revised January 19, 1999; accepted January 20, 1999